# Impact of Physiological Characteristics on Thermal Comfort of Cycling Helmet

Zixiang Hu<sup>o</sup>a, Xiaoyi Cai<sup>o</sup>b and Peng Zhou<sup>o</sup>c

Department of Mechanical and Aerospace Engineering, The Hong Kong University of Science and Technology, Clear Water Bay, Kowloon, Hong Kong SAR, China

Keywords: Cycling Helmet, Thermal Comfort, Physiological Characteristics, Convective Heat Transfer.

Abstract:

Research on helmet thermal comfort is crucial for optimizing helmet design and enhancing cyclists' acceptance of helmets. However, existing studies often neglect the impact of cyclists' physiological characteristics on scalp heat dissipation details. To address this gap, a sweating thermal mannequin head was developed to investigate the effects of physiological factors, including hair, sweating, and variations in head pitch angle, on scalp heat dissipation at typical cycling speeds. The findings reveal that hair obstructs airflow within the helmet, resulting in local thermal discomfort at the back of the scalp and potentially altering the optimal pitch angle for helmet thermal performance. Moreover, sweating amplifies the temperature differences between local "hot spots" and "cold spots" on the scalp, with the majority of heat loss attributed to sweat evaporation. Additionally, adjusting the pitch angle can better align the ventilation holes with the airflow, thereby enhancing thermal comfort at both the front and back of the scalp.

#### 1 INTRODUCTION

Head injury is a leading cause of serious injuries in cycling (Wood and Milne, 1988), and the use of cycling helmets has been shown to significantly reduce the risk of such injuries (Olivier and Creighton, 2017; Cripton et al., 2014). However, the head is highly sensitive to heat due to its critical role in regulating both brain and body temperature (Gerrett et al., 2014). Prolonged cycling in elevated ambient temperatures can result in overheating of the head, leading to thermal discomfort, which is a primary reason cyclists may choose not to wear helmets (Bogerd et al., 2015). Therefore, research on thermal comfort in cycling helmets can help optimize the ventilation design, thereby increasing cyclists' acceptance of the helmet.

The head is the most temperature-sensitive region of the human body (Kim et al., 2017). At the same temperature, individuals tend to experience greater discomfort from heat on the head compared to other body parts (Mehrabyan et al., 2011). Fang et al. (2018) conducted experiments with subjects and found that sensitivity to temperature varies across different locations on the scalp, and the presence of hair

will suppress this sensitivity. During cycling, the influence of the helmet can lead to heat accumulation on the scalp of the cyclist, resulting in thermal discomfort. In previous research, thermal comfort analysis of helmets is primarily conducted using thermal mannequin heads with heating and temperature feedback functions in wind tunnel experiments (Alam et al., 2010).

Helmet thermal comfort evaluation typically employs convective heat transfer parameters for characterization. Thermal resistance and heat transfer coefficient (Zwolińska et al., 2014; Youssef et al., 2019) are used to assess the cooling capacity of helmets in non-sweating conditions, calculated based on scalp area, temperature difference between the head and environment, and heat loss through the scalp. As cyclists inevitably encounter hot weather and perspire during outdoor riding, evaporative resistance (Aljaste et al., 2015; Pang et al., 2014) is used to evaluate helmet thermal performance in sweating conditions. The aforementioned studies provided only global parameter values of helmets, typically obtained under low wind speeds below 4 m/s. However, parameters such as thermal resistance and evaporative resistance exhibit significant sensitivity to wind speed. Mukunthan et al. (2019) observed a 20% reduction in helmet global thermal resistance when wind speed increased from 3 m/s to 6 m/s. Wind speed may exert non-negligible influence on thermal comfort studies

<sup>&</sup>lt;sup>a</sup> https://orcid.org/0009-0005-5227-9888

b https://orcid.org/0009-0005-4430-8095

<sup>&</sup>lt;sup>c</sup> https://orcid.org/0000-0003-4936-9661

of helmets.

Previous studies have investigated local thermal comfort in different regions of the head. Bruhwiler et al. (2003) utilized a commercially available thermal manikin head to partition the head into two regions (scalp and face) for comparing convective heat transfer coefficients under varying wind speeds. Martínez et al. (2016) further subdivided the scalp into six regions for similar investigations. The limited deployment of only one temperature sensor per region proves insufficient for detailed scalp thermal analysis, consequently hindering precise correlation between helmet ventilation configuration (vent holes and air channels) and local thermal comfort.

Additionally, previous studies have also investigated the influence of cyclists' physiological characteristics on helmet thermal comfort evaluation, including hair (Abeysekera and Shahnavaz, 1990), sweating (Mukunthan et al., 2019), and head pitch angle (Alam et al., 2005). Aljaste et al. (2015) compared the thermal resistance values of different helmets with and without hair to assess the effect of hair on thermal comfort. However, Bogerd and Bruhwiler (2008) found that 40%-50% of the reduction in convective heat transfer was caused by the hair-fixing layer, meaning that hair thickness, material, and thermal properties of the layer all influence experimental results. Brühwiler et al. (2003) tested and compared the convective heat loss of multiple helmets in both sweating and non-sweating states, while Mustary et al. (2014) compared scalp surface temperature differences among different helmets at three head pitch angles. Nevertheless, these studies treated the helmet as a whole and defined its thermal comfort through a global parameter, neglecting the heat dissipation details of the scalp, thus failing to reveal the influence of these three physiological characteristics on helmet thermal performance from the perspective of local thermal comfort.

In this study, a sweating thermal mannequin head was developed to investigate the influence of cyclists' physiological characteristics on the assessment of global and local thermal comfort in helmets. Wind tunnel experiments were conducted on four commercial helmets and one helmet prototype at a typical cruising speed (9m/s) of cyclists. The details of scalp heat dissipation were investigated, and the effects of physiological characteristics such as hair, sweating, and adjustments in head pitch angle on the assessment of helmet thermal comfort were analyzed.

# 2 METHODOLOGY

#### 2.1 Thermal Mannequin Head

To investigate the influence of physiological characteristics on the heat dissipation details and local thermal comfort of helmets, a thermal mannequin head was developed to simulate hair, sweating, and variations in head pitch angle. The thickness of the thermal head scalp is 10 mm, and the material is a photocurable resin with a thermal conductivity of  $0.2 \, \text{W/(m\cdot K)}$ , similar to that of human scalp (Baldry et al., 2018).

The upper section of the thermal head, functioning as the heating component, is equipped with a PID temperature control system to precisely elevate scalp surface temperature to predetermined levels. The overall heat loss of the system is measured by a power meter with an accuracy of 1%, and the temperature variation on the scalp's outer surface is maintained within 2 °C under still air conditions, consistent with actual human conditions (Kublanov et al., 2020). Ttype thermocouple is used for temperature measurement, with a probe diameter of less than 0.5 mm and a waterproof design, facilitating temperature collection under sweating conditions. Additionally, Sweat simulation is achieved using a syringe pump, which utilizes a high-precision step motor and gear reducer to expel water from the syringe at a predetermined

The lower part of the thermal head functions as the mechanical connection section, enabling head pitch angle control via a step motor. An insulating pad is placed between the upper and lower sections of the head, as indicated by the black line in Figure 1b, to ensure that all heat dissipates from the upper section. The head pitch angle  $\alpha$  is defined as the angle between the insulating pad and the horizontal direction, with a downward inclination being considered negative.

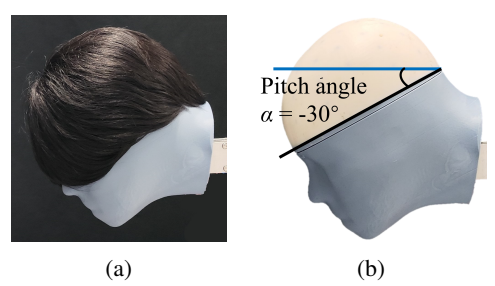


Figure 1: Thermal mannequin head: (a) hair simulation (b) pitch angle definition.

The thermal experiment is conducted using the developed sweating thermal head. The thermal head is positioned in front of an open-jet wind tunnel, with a

Table 1: Thermal mannequin head specifications.

Item	Values
Heat loss sampling frequency	1 Hz
Heat loss sampling accuracy	1 %
Temperature sampling frequency	1 Hz
Temperature sampling accuracy	$0.5^{\circ}\mathrm{C}$
Temperature sampling resolution	$0.01^{\circ}\mathrm{C}$
Syringe pump accuracy	$\leq 0.5\%$



Figure 2: Experimental setup.

blockage ratio of 0.05. A wind speed of 32.4 km/h (9 m/s) was selected to represent the typical velocity of a cyclist.

# 2.2 Helmet Samples

Four commercially available professional-grade road cycling helmets were tested in this study. Due to the complex configurations of ventilation holes and air channels in these commercial helmets, which exhibit strong interdependencies, it is necessary to reduce the number of ventilation holes and air channels to investigate the influence of physiological characteristics on helmet thermal performance under a simpler vent configuration. Therefore, a helmet prototype with adjustable ventilation hole positions and air channel depths, created through 3D printing, was also used for wind tunnel experiments.

The helmet prototype consists of an outer shell, an inner shell, ventilation hole walls, and insulation filling material, which effectively suppresses the conductive heat transfer between the thermal head and the air. As shown in Figure 4b, under stable natural convection conditions, the outer surface temperature of the helmet prototype is generally consistent with the air temperature. Both the inner and outer shells, as well as the walls of the ventilation holes, are produced using 3D printing and undergo surface treatment, which includes polishing and applying matte paint, to simulate the material properties of actual helmet surfaces. The helmet can simulate different depths of air channels by replacing the inner shell with different designs.



Figure 3: Tested road cycling helmets: (a) helmet 1 (b) helmet 2 (c) helmet 3 (d) helmet 4.

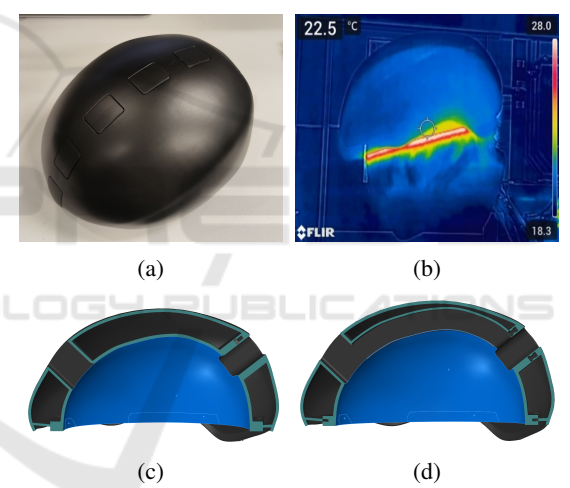


Figure 4: 3D printed helmet prototype: (a) model structure (b) thermal insulation performance (c) 0 mm air channel depth (d) 20 mm air channel depth.

#### 2.3 Experimental Procedures

The experimental procedure comprised the following key steps: First, the heating device was turned on to elevate the scalp surface temperature to 35°C to simulate human thermal physiology, while the ambient temperature is 20.5°C. Data acquisition equipment was initiated to record the scalp surface temperature, heat loss dissipated from the head, and ambient temperature and humidity, establishing a baseline with the stabilized scalp surface temperature. The test helmet was placed on the head, allowing the scalp surface temperature to stabilize again. The wind tunnel was then turned on with wind speed adjusted to 9

m/s. After stabilization, the scalp surface temperature was compared to the baseline to evaluate temperature drops at various scalp locations. The final temperature drop results were mapped onto a plane to visualize local heat dissipation details. Finally, the global thermal resistance, global evaporative resistance, and convective heat transfer coefficient were calculated.

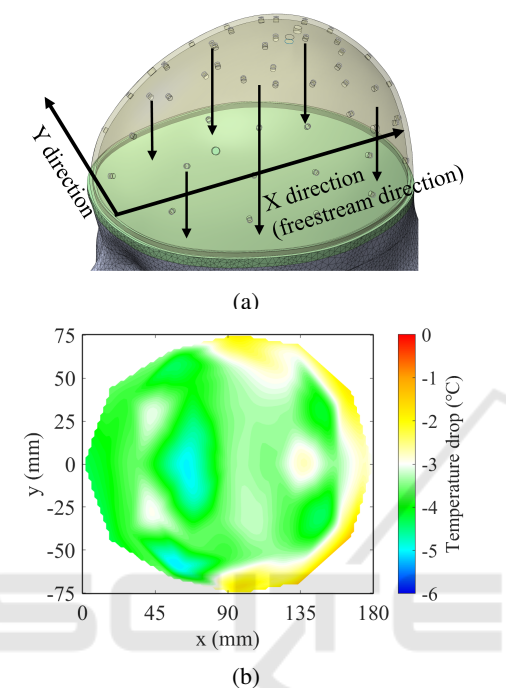


Figure 5: Visualization of scalp surface temperature: (a) projection method (b) projection result.

The convective heat transfer coefficient h and global thermal resistance  $R_{ct}$  of helmets are calculated using the following formula:

$$h = \frac{1}{R_{\rm ct}} = \frac{H_{\rm dry} - H_{\rm rad}}{A_{\rm scalp} \cdot (T_{\rm scalp} - T_{\rm air})},\tag{1}$$

where  $H_{\rm dry}$  and  $H_{\rm rad}$  denote the power supplied to the head and the heat dissipation from the scalp through thermal radiation, respectively.  $A_{\rm scalp}$  represents the scalp surface area, and  $T_{\rm scalp}$  and  $T_{\rm air}$  are temperatures of the scalp surface and the ambient environment, respectively.

The global evaporative resistance is calculated using the following formula:

$$R_{\rm et} = \frac{A_{\rm scalp} \cdot (p_{\rm scalp} - p_{\rm air})}{H_{\rm wet} - H_{\rm conv} - H_{\rm rad} - H_{\rm correct}},$$
 (2)

where  $p_{\text{scalp}}$  and  $p_{\text{air}}$  represent the saturated water vapor pressures at the scalp surface temperature and the air's water vapor pressure, respectively.  $H_{\text{conv}}$  and  $H_{\text{rad}}$  are the dry heat loss consisting of convective heat

and radiative heat loss, and  $H_{\text{correct}}$  is the inevitable heat loss owing to sweating conditions, caused by the temperature difference between the sweat in the syringe pump and on the scalp.

#### 3 RESULTS AND DISCUSSION

In this section, the effects of physiological characteristics such as hair, sweating, and changes in head pitch angle on the helmet thermal comfort were analyzed using the four commercial helmets mentioned above. Additionally, experiments were conducted using the helmet prototype with air channel depths of 0 mm and 20 mm under the same testing conditions, with the results serving to validate and complement the previous conclusions.

The upper part of the thermal head was made from suitable materials and thickness to simulate the thermal conductivity and thickness between the outer surface of the human scalp and the skull. The inner surface of the upper part is heated by a heating layer to optimally simulate the temperature regulation mechanism of the human scalp surface. In different comparative experiments, the temperature of the heating layer inside the thermal head was maintained at a constant level.

#### 3.1 Effect of Hair

The helmet 1 was tested under both conditions of having hair and being hairless, revealing scalp heat dissipation details in both scenarios, as shown in Figure 6. First, when the helmet's ventilation holes are connected to the air channels, air can more easily pass over the scalp, thereby removing heat and promoting local thermal comfort. This trend is observed regardless of whether hair is present or not.

In the hairless condition, air can more easily circulate in the gap between the scalp and the helmet, even if the air channel depth is relatively small. As shown in Figure 6a, the rear part of the scalp exhibits a local low-temperature area, with a temperature difference of only 1°C compared to the scalp surface temperature near the ventilation holes, indicating that airflow can reach this region within the helmet. However, when hair is present, this phenomenon disappears, replaced by a large high-temperature area at the back of the scalp, which is 3.5°C higher than the temperature near the ventilation holes, as shown in Figure 6b. This suggests that the presence of hair obstructs airflow within the helmet, resulting in local thermal discomfort at the rear.

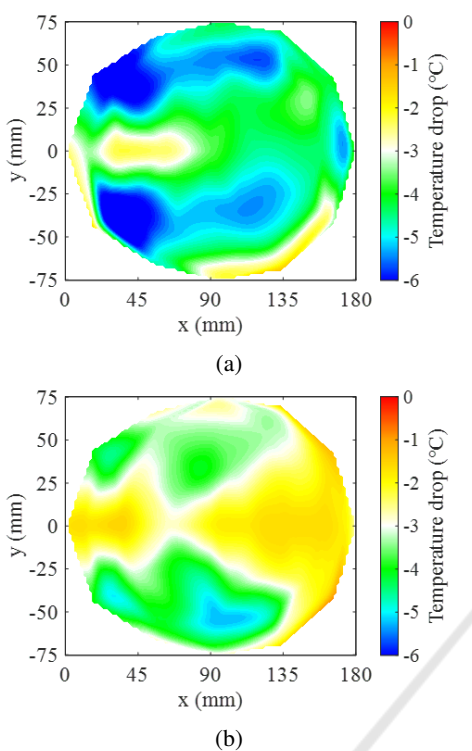


Figure 6: Heat dissipation details of helmet 1 under: (a) hairless condition (b) hair condition.

# 3.2 Effect of Sweating

The internal heating temperature of the thermal head is maintained at the same level in both the sweating and non-sweating experiments using a PID control method. The helmet 2 and helmet 3 were tested under both conditions, revealing scalp heat dissipation details in both scenarios, as shown in Figure 7 and Figure 8. The results indicate that while the heat dissipation patterns are similar in both sweating and non-sweating conditions, there is a significant temperature difference, reaching up to 7 °C. This highlights the substantial impact of sweating on heat dissipation. Additionally, although the patterns of heat dissipation are similar, the temperature differences between local "hot spots" and "cold spots" are amplified during the sweating condition.

Table 2: Heat loss of helmet 2 under non-sweating and sweating conditions

Item	Values
Total heat loss (non-sweating condition)	11.33 W
Total heat loss (sweating condition)	17.20 W
Sensible heat loss (sweating condition)	3.16 W
Latent heat loss (sweating condition)	14.04 W

Under sweating conditions, the total heat loss of

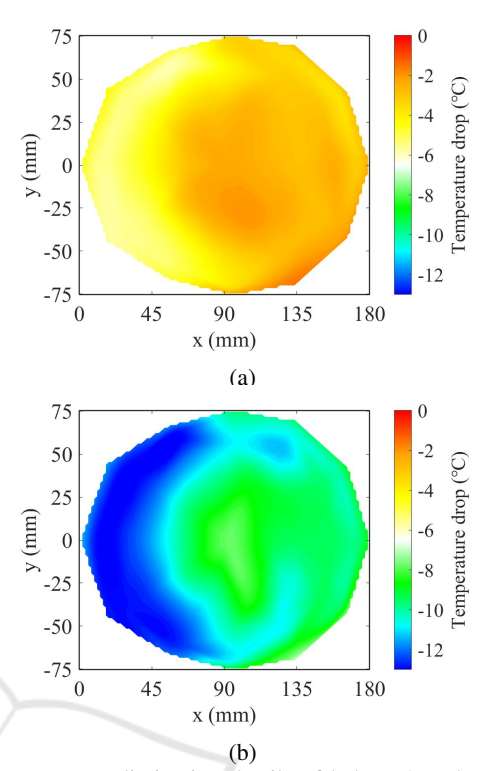


Figure 7: Heat dissipation details of helmet 2 under: (a) non-sweating condition (b) sweating condition.

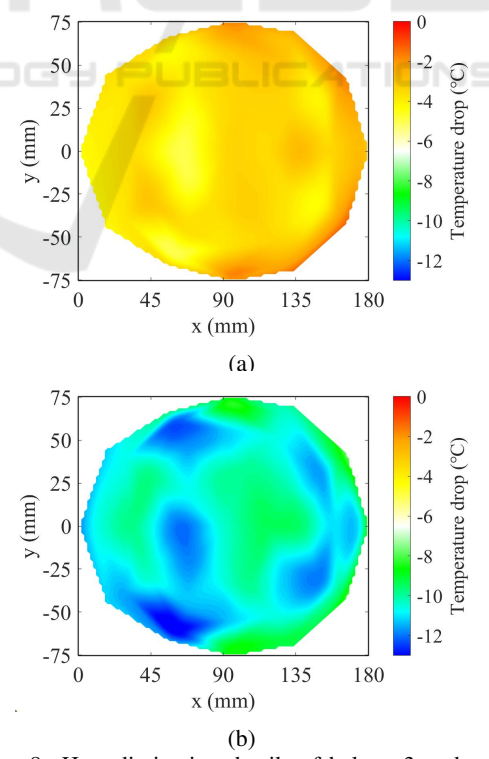


Figure 8: Heat dissipation details of helmet 3 under: (a) non-sweating condition (b) sweating condition.

helmet 2 reached 17.20 W, representing an increase of 51.7% compared to the non-sweating condition, with the latent heat loss reaching 14.04 W. This indicates that over 80% of the heat is dissipated through the evaporation of sweat, which corresponds to convective mass transfer.

#### 3.3 Effect of Head Pitch Angle

Helmet 4 was tested at two common head pitch angles used by cyclists: a normal angle  $(-10^{\circ})$  and a more aggressive angle  $(-30^{\circ})$ , under non-sweating conditions. The heat dissipation details reveal the differences, as shown in Figure 9. When the pitch angle is smaller, the orientation of the ventilation hole is more directly aligned with the incoming airflow, resulting in a larger low-temperature area at the front of the scalp. Additionally, air can more easily reach the back of the scalp, lowering the temperature in that area.

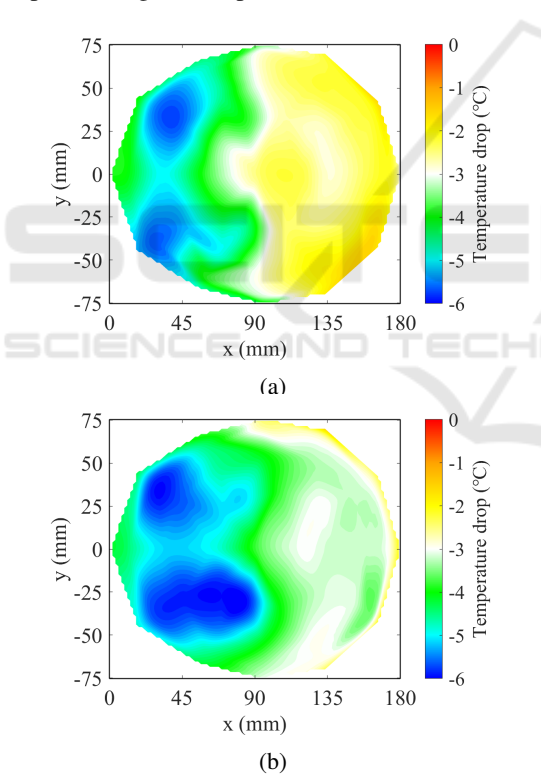


Figure 9: Heat dissipation details of helmet 4 in: (a) -10 °pitch angle (b) -30 °pitch angle.

The change in pitch angle results in a 10.2% reduction in the global thermal resistance of the helmet. Based on previous test results of different helmets at the same pitch angle, it can be observed that the difference in global thermal resistance values of the same helmet at different pitch angles can be greater than the differences in global thermal resistance values be-

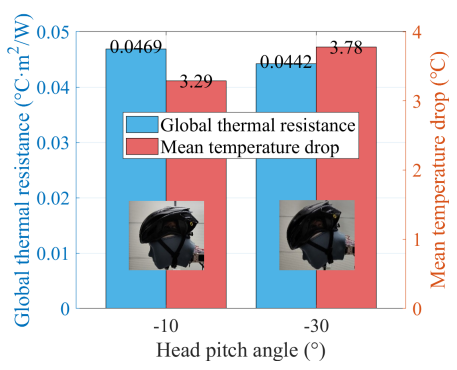


Figure 10: Comparison of global thermal resistance and mean temperature drop in different pitch angles.

tween different helmets. This demonstrates the significant impact of pitch angle on the global thermal comfort of helmets.

# 3.4 Helmet Prototype Experiment

The experimental setup for the helmet prototype is identical to that of the four commercial helmets. The wind tunnel experiment results clearly demonstrate the significant influence of hair on the internal airflow within helmets. For helmets with 0 mm air channel depth, air can still pass through the narrow gap between the scalp and helmet inner surface in hairless conditions. However, the presence of hair substantially impedes internal airflow circulation. This restriction limits heat transfer primarily to impingement cooling from the frontal ventilation hole, while causing significant heat accumulation in the rear region. Such uneven thermal distribution ultimately leads to pronounced thermal discomfort for the cyclist.

In the case of 20 mm air channel depth, when there is no hair, air can smoothly flow along the air channel to the back of the scalp, thereby enhancing the convective heat transfer at the rear. However, when hair is present, the difficulty of airflow along the air channel significantly increases, and in certain pitch angles, the air channel's contribution to convective heat transfer is not very pronounced.

Pitch angle also has a substantial impact on the thermal performance of the helmet. For 0 mm air channel depth, in the absence of hair, a decrease in pitch angle results in a noticeable increase in the "cool region" at the front of the scalp and a corresponding increase in the "hot region" at the back of the scalp. Similarly, the same conclusion can be drawn when hair is present.

In the case of 20 mm air channel depth, the situation is slightly different. In the absence of hair, as the pitch angle decreases, convective heat transfer increases, and the enhancing effect of the air channel

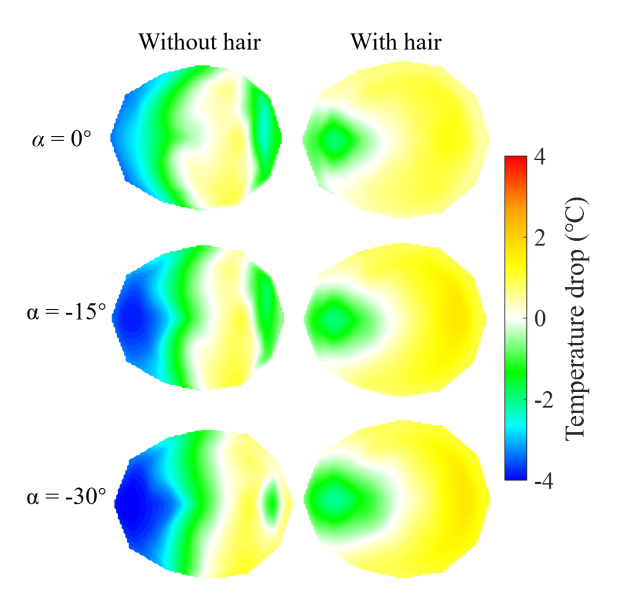


Figure 11: Experimental results of 0 mm depth air channel helmet prototype.

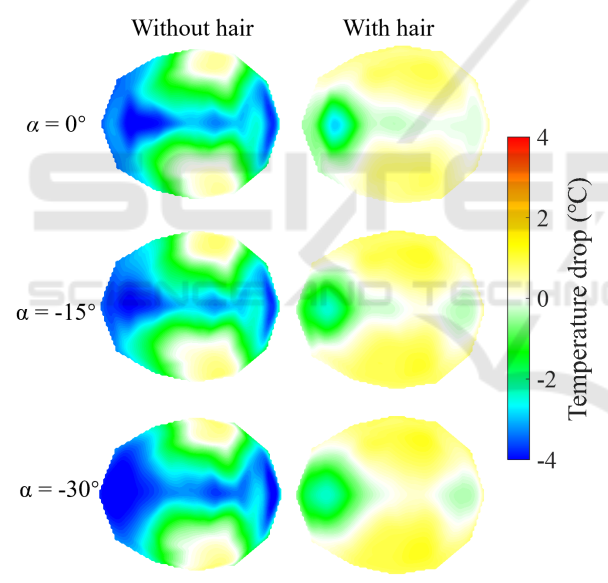


Figure 12: Experimental results of 20 mm depth air channel helmet prototype.

on heat dissipation can be clearly observed. However, when hair is present, the pattern is quite the opposite. As the pitch angle decreases, the effectiveness of the air channel diminishes, and the temperature remains low only at the front and rear areas close to the ventilation holes, indicating that the heat dissipation performance of the helmet at different pitch angles also depends on the presence of hair. The optimal pitch angle for a helmet differs between conditions with and without hair.

# 4 CONCLUSIONS

In this study, a sweating thermal mannequin head was developed, and four commercial helmets along with one prototype were used to investigate the effects of physiological characteristics, including hair, sweating, and variations in head pitch angle, on scalp heat dissipation. The conclusions can be effectively applied to the thermal comfort optimization of helmet design, thereby enhancing cyclists' acceptance and wearing compliance. The main conclusions are as follows:

The hair filling the gap between the scalp and helmet inner surface significantly alters the internal airflow patterns compared to hairless conditions, often inducing local thermal discomfort at the rear region. Furthermore, the presence or absence of hair modifies the optimal pitch angle for helmet thermal performance.

Sweating enhances the helmet's overall thermal comfort while simultaneously amplifying temperature differentials between localized "hot spots" and "cold spots" on the scalp. It also suppresses sensible heat transfer, resulting in the majority of heat dissipation being attributable to sweat evaporation.

Adjusting the pitch angle alters the ease of airflow entry through ventilation holes into the helmet interior, significantly affecting local thermal comfort of the scalp, particularly in the rear region.

#### **ACKNOWLEDGEMENTS**

This work is partially supported by the Hong Kong Innovation and Technology Commission (No. ITS/101/23FP). The study was conducted in the Aerodynamics Acoustics & Noise Control Technology Centre (aantc.ust.hk).

# **REFERENCES**

Abeysekera, J. D. and Shahnavaz, H. (1990). Adaptation to discomfort in personal protective devices: an example with safety helmets. *Ergonomics*, 33(2):137–145.

Alam, F., Chowdhury, H., Elmir, Z., Sayogo, A., Love, J., and Subic, A. (2010). An experimental study of thermal comfort and aerodynamic efficiency of recreational and racing bicycle helmets. *Procedia Engi*neering, 2(2):2413–2418.

Alam, F., Watkins, S., and Subic, A. (2005). Aerodynamic efficiency and thermal comfort of bicycle helmets. In *Proc. of the 6th International Conference on Mechanical Engineering (ICME2005)*, pages 28–30. ICME. TH-32 (1–6).

- Aljaste, H., Kuklane, K., and Heidmets, S. S. (2015). The effects of air channel construction and design elements on heat transfer characteristics of bicycle helmets for commuters. In 4th International Cycling Safety Conference, Medizinische Hochschule Hannover, Germany. ICSC.
- Baldry, M., Timchenko, V., and Menictas, C. (2018). Thermal modelling of controlled scalp hypothermia using a thermoelectric cooling cap. *Journal of Thermal Biology*, 76:8–20.
- Bogerd, C. P., Aerts, J. M., Annaheim, S., Bröde, P., De Bruyne, G., Flouris, A. D., and Rossi, R. M. (2015). A review on ergonomics of headgear: Thermal effects. *International Journal of Industrial Ergonomics*, 45:1–12.
- Cripton, P. A., Dressler, D. M., Stuart, C. A., Dennison, C. R., and Richards, D. (2014). Bicycle helmets are highly effective at preventing head injury during head impact: Head-form accelerations and injury criteria for helmeted and unhelmeted impacts. Accident Analysis & Prevention, 70:1–7.
- Gerrett, N., Ouzzahra, Y., Coleby, S., Hobbs, S., Redortier, B., Voelcker, T., and Havenith, G. (2014). Thermal sensitivity to warmth during rest and exercise: a sex comparison. *European Journal of Applied Physiology*, 114:1451–1462.
- Kim, Y. B., Jung, D., Park, J., and Lee, J. Y. (2017). Sensitivity to cutaneous warm stimuli varies greatly in the human head. *Journal of Thermal Biology*, 69:132–138
- Kublanov, V. S., Borisov, V. I., and Babich, M. V. (2020). Simulation the distribution of thermodynamic temperatures and microwave radiation of the human head. Computer Methods and Programs in Biomedicine, 190:105377.
- Mehrabyan, A., Guest, S., Essick, G., and McGlone, F. (2011). Tactile and thermal detection thresholds of the scalp skin. *Somatosensory & Motor Research*, 28(3–4):31–47.
- Mukunthan, S., Vleugels, J., Huysmans, T., Kuklane, K., Mayor, T. S., and De Bruyne, G. (2019). Thermal-performance evaluation of bicycle helmets for convective and evaporative heat loss at low and moderate cycling speeds. *Applied Sciences*, 9(18):3672.
- Olivier, J. and Creighton, P. (2017). Bicycle injuries and helmet use: a systematic review and meta-analysis. *International Journal of Epidemiology*, 46(1):278–292.
- Pang, T. Y., Subic, A., and Takla, M. (2014). Evaluation of thermal and evaporative resistances in cricket helmets using a sweating manikin. *Applied Ergonomics*, 45(2):300–307.
- Wood, T. and Milne, P. (1988). Head injuries to pedal cyclists and the promotion of helmet use in victoria, australia. *Accident Analysis & Prevention*, 20(3):177–185
- Youssef, A., Colon, J., Mantzios, K., Gkiata, P., Mayor, T. S., Flouris, A. D., and Aerts, J. M. (2019). Towards model-based online monitoring of cyclist's head thermal comfort: smart helmet concept and prototype. *Applied Sciences*, 9(15):3170.

Zwolińska, M., Bogdan, A., and Fejdyś, M. (2014). Influence of different types of the internal system of the ballistic helmet shell on the thermal insulation measured by a manikin headform. *International Journal of Industrial Ergonomics*, 44(3):421–427.